Progress In Electromagnetics Research Letters, Vol. 110, 117–126, 2023

MIMO Antenna with Reduced Mutual Coupling Using Circular Ring Neutralization Structure

Kondapalli Venu Gopal* **and Yarravarapu Srinivasa Rao**

Abstract—In this article, a $15 \times 20\,\text{mm}^2$ arbitrary-shaped antenna is built. The same is extended to a 2×2 MIMO antenna with size $32 \times 20\,\text{mm}^2$. It covers two bands. Band-1 covers 3–4.44 GHz, and band-2 covers 5.32–11.1 GHz. In this case, a circular neutralization structure is used to lessen the mutual coupling between the two ports. The ECC, DG, CCL, and radiation pattern are used to demonstrate how well the MIMO antenna performs. Also, it has been noted that there is good agreement between simulated and measured outcomes.

1. INTRODUCTION

An antenna array is essential in microwave communications that demand wide coverage. Transceivers with several bands are necessary for modern communication. A mobile phone can be used for a variety of things, including voice communication, data transfer, GPS, Bluetooth, and Wi-Fi. One antenna takes up more room and performs worse when it is utilized for just one application. The usage of identical antennas provides a fix for this and enhances radiation performance in general. However, the issue is that every electronic device has relatively little area designated for antennas. When multiple antennas placed near together, interaction between electromagnetic fields occurs. This phenomenon is known as mutual coupling (MC). Mutual coupling has a detrimental effect on multiple-input multiple-output (MIMO) antenna performance. Numerous antenna parameters, including impedance, received voltages, and radiation patterns, are altered. The MIMO antenna components are anticipated to function separately and with significant isolation under these circumstances. Consequently, it is essential to lessen MC's impact.

In [1] a multi-band MIMO antenna is designed, and MC is minimized using defected ground structure (DGS) and parasitic elements. In [2], MC between the elements is reduced using parametric approach of distance parameter. In [3–5], MC between the elements is reduced using a neutralization line. In [6], MC is reduced using a decoupling network. In [7, 8], MC is reduced using reconfigurable radiation pattern and reconfigurable intelligent surfaces. In [9], MC is reduced using complementary split ring resonator (CSRR) structures.

2. ANTENNA CONFIGURATION

Figure 2 depicts the proposed antenna's geometry and size. The proposed antenna is developed on an FR-4 substrate with $\varepsilon_r = 4.4$ and $\delta = 0.02$. The designing procedure of the antenna is described in the following steps.

Step-1: Take a circular cylinder with radius 3 mm and take another circular cylinder with radius 3 mm with 4 segments rhombus and then intersect.

Received 15 April 2023, Accepted 23 April 2023, Scheduled 2 June 2023

* Corresponding author: Kondapalli Venu Gopal (venugopal.kondapalli@gmail.com).
The authors are with the Department of Instrument Technology, Andhra University, Visakhapatnam, AP, India.

Step-2: It is 30° rotated.

Step-3: Take another circular ring with outer radius 3.5 mm and inner radius 3.3 mm and subtracted as shown in Figure 1.

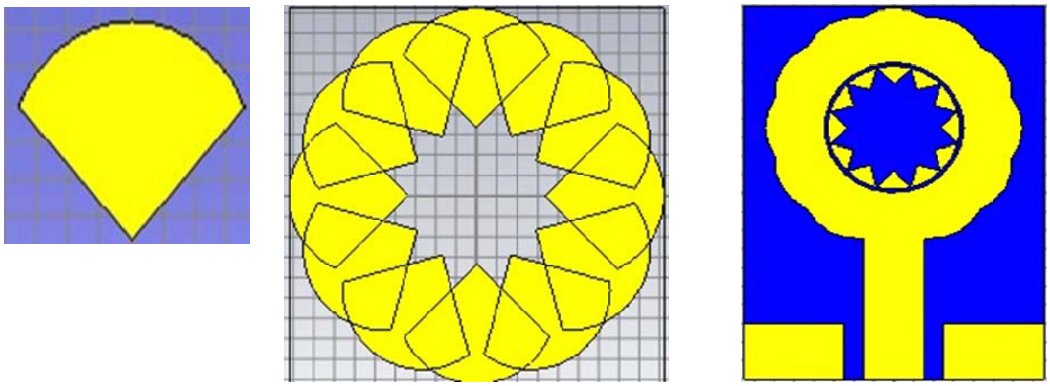

Figure 1. Evolution of the antenna.

The patch's overall size is $0.12\lambda_0 \times 0.19\lambda_0$. In Table 1, the antenna's optimal parameters are displayed.

Table 1. Parameters of the proposed antenna.

Parameter	W_s	L_s	H_s	W_F	A	B	R	R_1
Units (mm)	15	20	1.4	3	5	3	6.14	3.5 outer 3.3 Inner

2.1. Return Loss

The return loss curve (S_{11}) of the suggested antenna is shown in Figure 3. The recommended antenna operates between the frequencies of 2.6–3.5 GHz and 5.66–10.8 GHz. The given antenna is appropriate for ultra-wideband (UWB) applications.

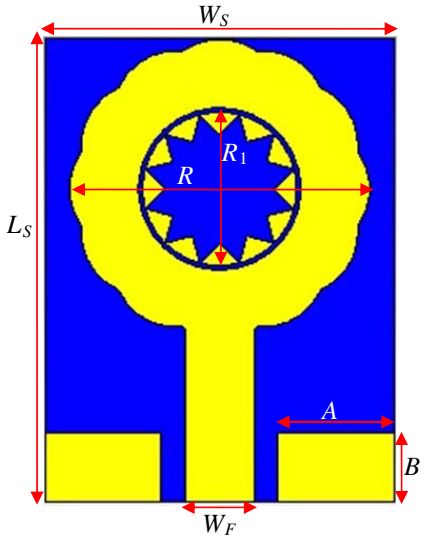

Figure 2. Proposed antenna.

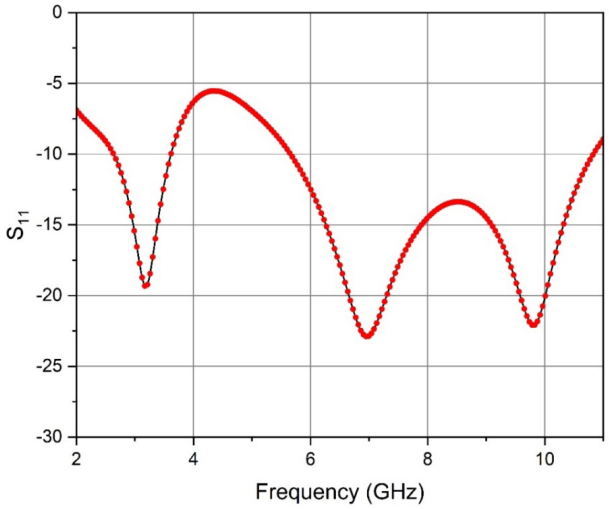

Figure 3. Return loss curve.

3. MIMO ANTENNA

The 2×2 MIMO antenna utilizes the same aerial. In regard to the origin, two patch antennas are symmetrically placed. Edge to edge, the distance between the two sections is 2 mm. The MIMO antenna is shown in Figure 4. Neutralization ring with outer radius 2.2 mm and inner radius 1.5 mm is taken. Table 2 displays the MIMO antenna's suitable specifications.

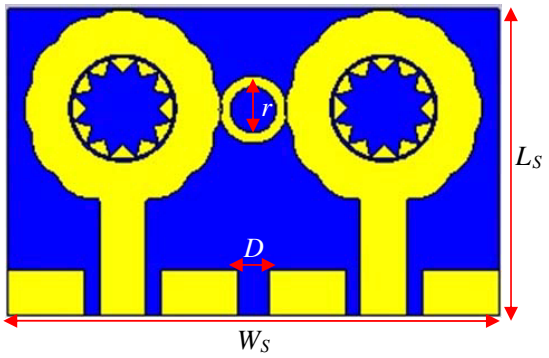

Figure 4. MIMO antenna.

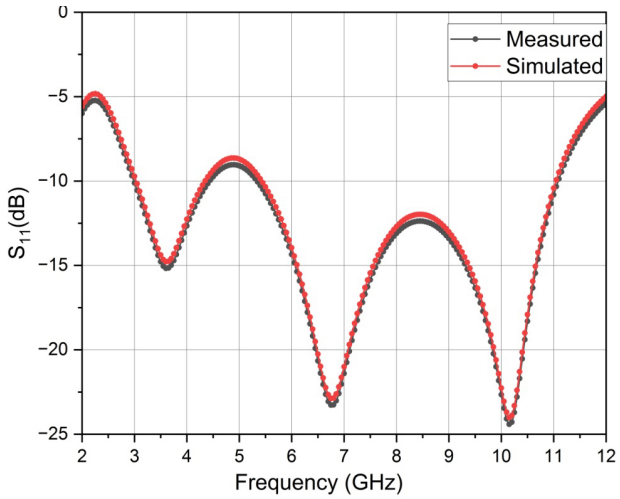

Figure 5. Return loss.

Table 2. The designed antenna's details.

Parameter	W_s	L_s	D	r
Units (mm)	32	20	2	2.2 1.5

3.1. Return Loss

The measured and simulated return loss curves are illustrated in Figure 5 for the suggested MIMO antenna. It covers two bands. Band-1 covers 3–4.44 GHz, and band-2 covers 5.32–11.1 GHz.

3.2. Mutual Coupling

Mutual coupling is the key performance indicator for the MIMO antenna. When two antennas are placed in the close proximity, mutual coupling arises between them. It is necessary to reduce MC since it has a negative impact on the performance of the MIMO antenna. Measured and simulated S_{21} for the proposed MIMO antenna are shown in Figure 6. It is observed that MC is below −15 dB in both bands.

In order to get physical insight of the mutual coupling between the elements, surface currents are observed at 3.59 GHz, 6.76 GHz, and 10.16 GHz. The circular ring prevents the propagation of surface currents from one element to another as shown in Figure 7. Port 1 is excited, and port 2 is terminated.

In Figure 8, the MC for the proposed MIMO antenna with and without the NR ring is displayed. It is noticed that without neutralization (NR) ring the MC is high in the highlighted region from 3 to 6 GHz. Inserting the NR ring between the elements reduces the MC below −15 dB over the two bands. It is observed that without NR in band 2 MC is below −15 dB due to pattern diversity as shown in Figure 9.

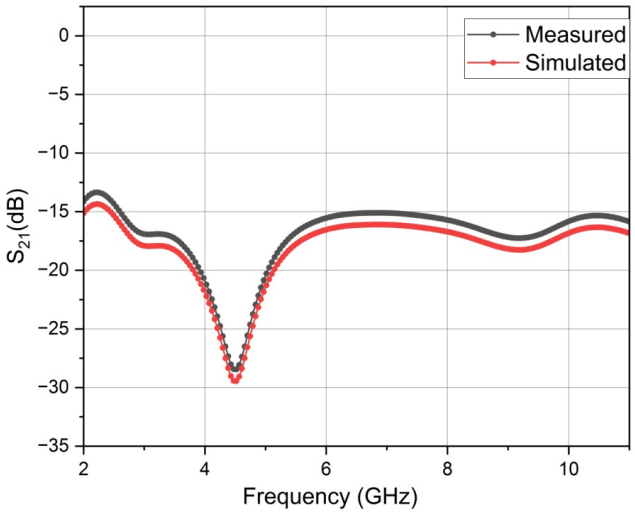

Figure 6. Mutual coupling.

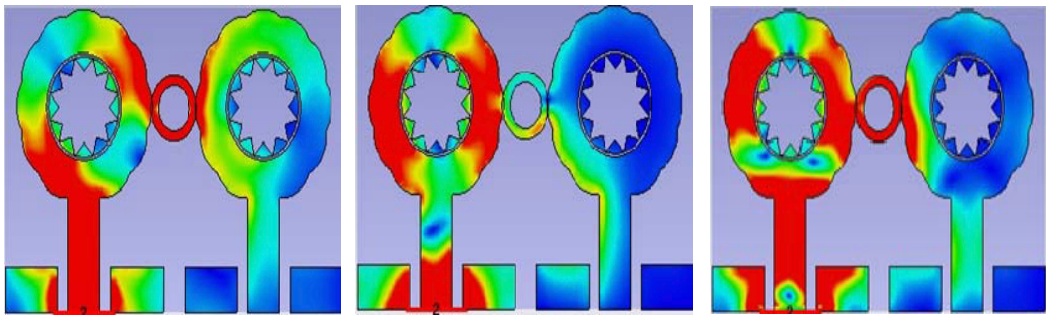

Figure 7. Surface current distribution at (a) 3.59 GHz, (b) 6.76 GHz, (c) 10.16 GHz.

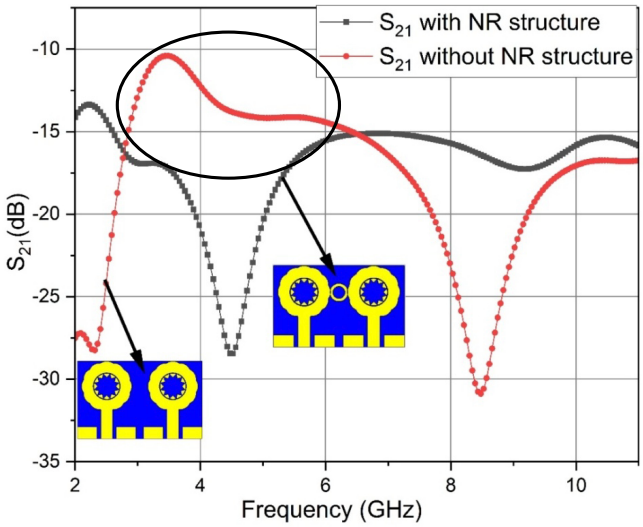

Figure 8. S_{21} with & without circular NR ring.

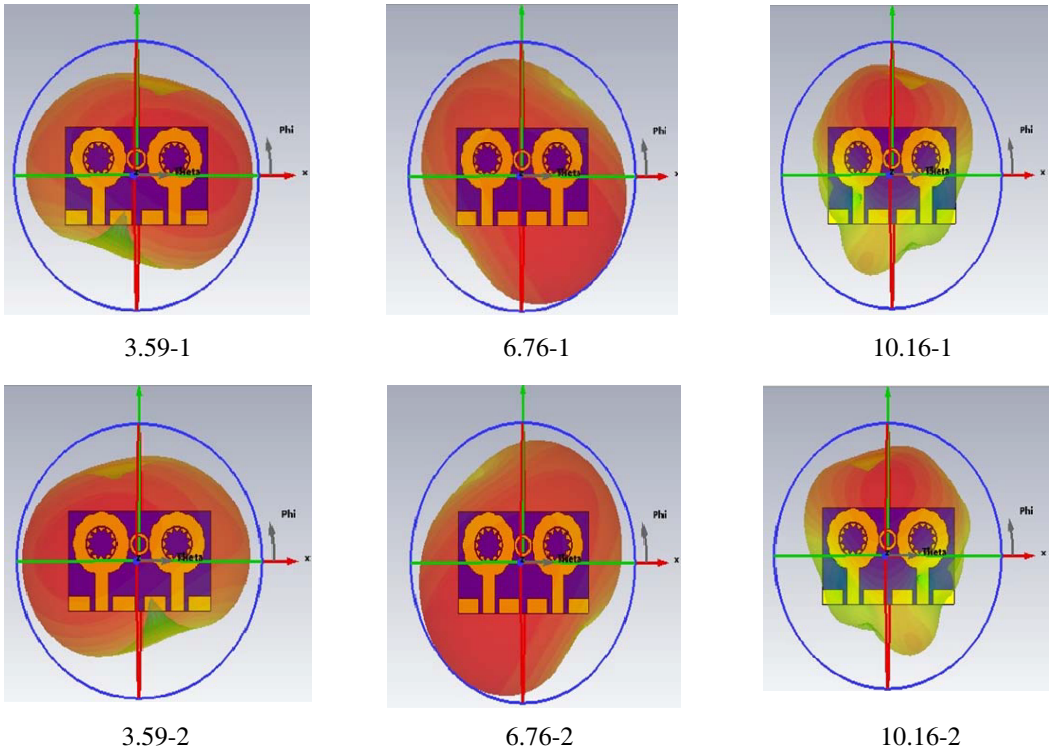

Figure 9. 3-D radiation patterns of the antenna upper row port-1 excited and lower row port-2 excited.

In Figure 10, the antenna's radiation patterns in the E-plane and H-plane are represented. The simulated (----) and measured (----) radiation patterns are similar. The fabricated prototype of the proposed antenna is shown in Figure 11.

The antenna under test (AUT) is connected to the SMA connector and attached to the ground plane with a width of 3 mm. Using Agilent 2-port connected PNA-L Network Analyzer the input impedance of in free space of AUT Z_{in} is measured. Next step is to fix the screws to the ground plane and attach the cap. Measure the impedance of AUT (Z_{wc}) using the Vector Network Analyzer. Finally, the ratio of real part differences of Z_{in} and Z_{wc} to the real part of Z_{in} got the radiation efficiency. It is noticed that there is an increase in the frequency of cross-polarized magnitude because of horizontal components increases. A proper placement of monopoles maintaining $\lambda/2$ separation reduces the mutual coupling.

The performance of MIMO antenna can be assessed using diversity gain, multiplexing efficiency, effective diversity gain, channel capacity loss, and envelope correlation coefficient.

3.2.1. Diversity Gain

Equation (1) can be used to compute the MIMO antenna's diversity gain. At 3.59 GHz, 6.76 GHz, and 10.16 GHz, the MIMO antenna's diversity gain (DG) is 9.98 dB, 9.99 dB, and 9.99 dB, respectively. DG plot is shown in Figure 12.

$$\mathrm{DG} = 10\sqrt{1 - |\mathrm{ECC}|^2} \tag{1}$$

3.2.2. Multiplexing Efficiency

Equation (2) is used to compute the multiplexing efficiency and total efficiency for a two element antenna.

$$|\rho_e|^2 = 1 - \frac{\eta_{mux}}{\eta_1 \eta_2} \tag{2}$$

The total efficiencies of antennas 1 and 2 are η_1 and η_2. η_{mux} is multiplexing efficiency.

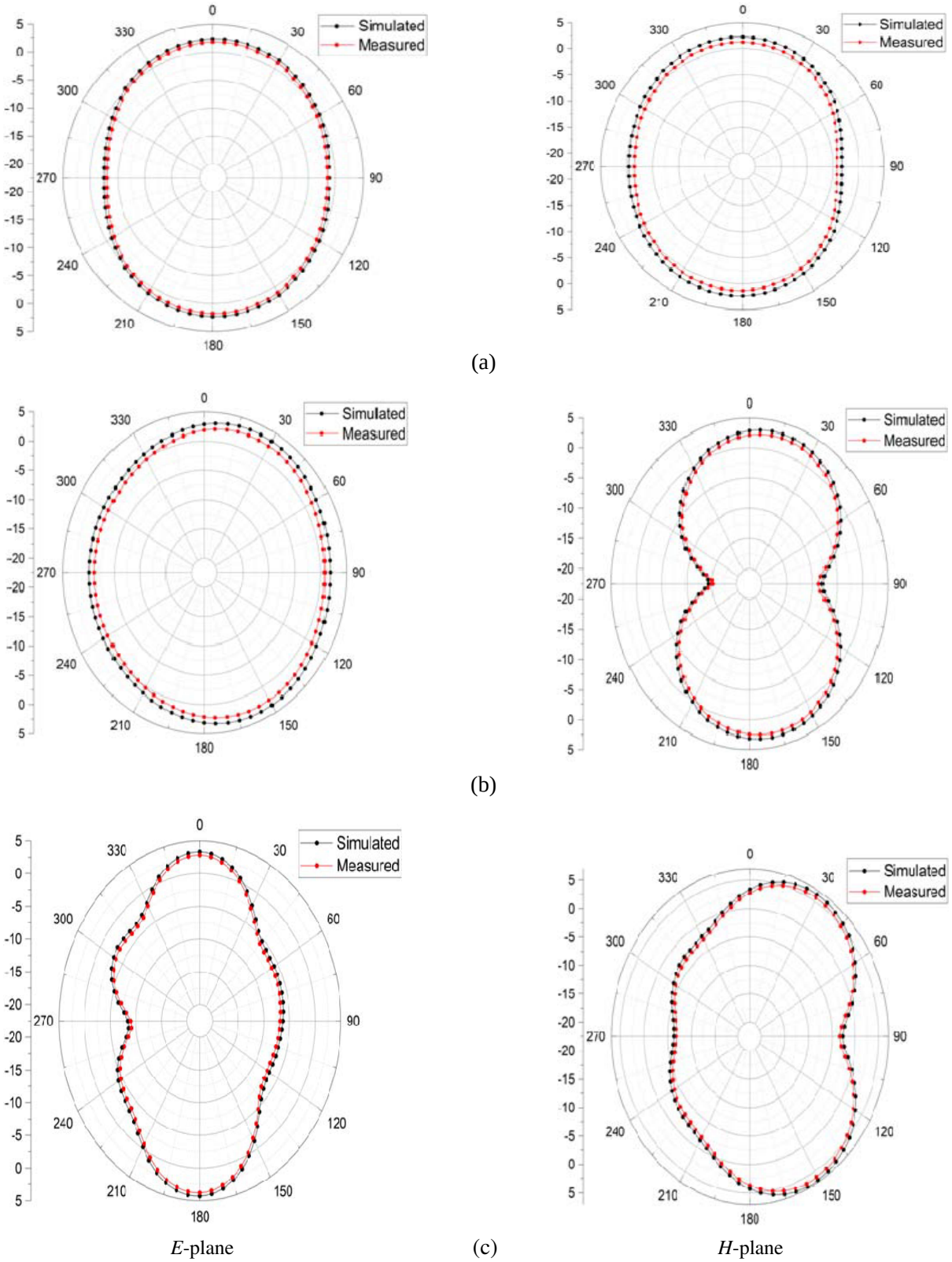

Figure 10. Measured and simulated radiation patterns in both E-plane and H-plane (a) 3.59 GHz, (b) 6.76 GHz, (c) 10.16 GHz.

(a) (b) (c)

Figure 11. Fabricated prototype. (a) Front view. (b) S-parameters measurement using VNA. (c) Radiation pattern measurement in anechoic chamber.

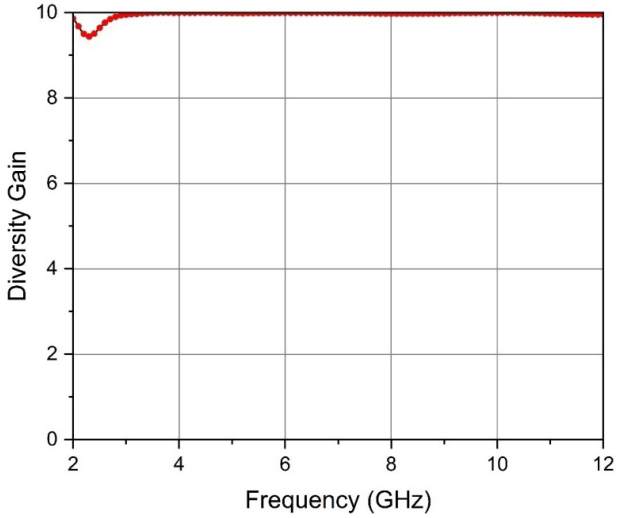

Figure 12. Diversity gain.

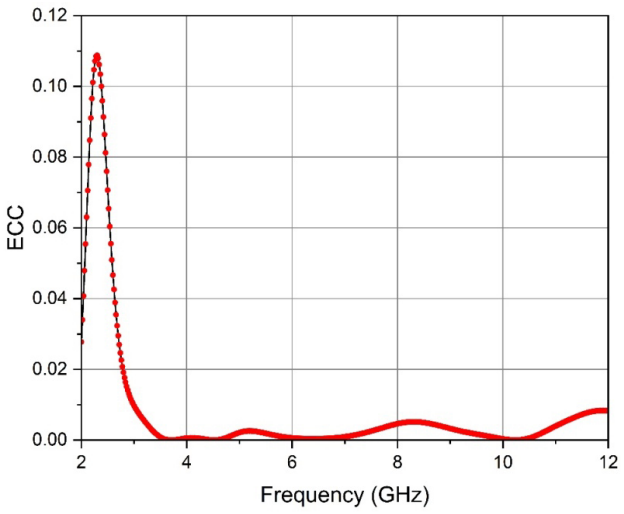

Figure 13. ECC.

3.2.3. Effective Diversity Gain

The antenna efficiency, DG, and effective diversity gain (EDG) relation is

$$\text{EDG} = \text{DG} \times \eta_{ant} \tag{3}$$

3.2.4. Channel Capacity Loss (CCL)

One of the key performance indicators for MIMO antennas is channel capacity. Figure 13 shows a graph of channel capacity loss. CCL can be calculated using Equation (5).

$$C_{\text{loss}} = -\log_2 \det(\Psi^R) \tag{4}$$

$$\Psi^R = \begin{bmatrix} \rho_{11} & \rho_{12} \\ \rho_{21} & \rho_{22} \end{bmatrix}$$

$$\rho_e = \frac{\left|s_{11}^* s_{12} + s_{21}^* s_{22}\right|^2}{\left(1 - |s_{11}|^2 - |s_{21}|^2\right)\left(1 - |s_{22}|^2 - |s_{12}|^2\right)} \tag{5}$$

with $\rho_{ii} = (1 - (|S_{ii}|^2 + |S_{ij}|^2))$ and $\rho_{ij} = -(S_{ii}^* S_{ij} + S_{ji}^* S_{jj})$ for $i, j = 1$ or 2.

3.2.5. Envelope Correlation Coefficient (ECC)

One of the most crucial variables to take into account when assessing a MIMO antenna's performance is ECC. Always maintain a lower correlation between the two sections. Diversity gain and ECC go hand in hand. The higher the DG is, the lower the ECC is. Figure 13 depicts the proposed MIMO antenna's envelope correlation coefficient curve, which can be calculated from fields using Equation (6).

$$\rho_c = \frac{\int_0^{2\pi}\int_0^{\pi} XPRE_{\theta K}(\theta,\emptyset)\, E^*_{\theta l}(\theta,\emptyset)\, P_\theta(\theta,\emptyset) + E_{\emptyset k}(\theta,\emptyset)\, E^*_{\emptyset l}(\theta,\emptyset)\, P_\emptyset(\theta,\emptyset)\sin\theta d\theta d\emptyset}{\sqrt{\sigma_k^2\sigma_l^2}} \tag{6}$$

The performance of the proposed antenna in terms of various parameters is shown in Table 3. The comparison of the proposed antenna with literature is shown in Table 4.

Table 3. Evaluation of the designed MIMO antenna's performance in terms of gain, mutual coupling, ECC, DG, multiplexing effectiveness, EDG and CCL.

Frequency/Parameter	3.59 GHz	6.76 GHz	10.16 GHz
Mutual coupling (dB)	−18	−16	−17
Efficiency	92	96	94
Gain	3.5	4.1	4
ECC	0.01	0.001	0.001
Diversity Gain	9.98	9.99	9.99
Multiplexing Efficiency	−0.11	−0.08	−0.05
Effective Diversity Gain	8.69	8.53	8.89
CCL	0.16	0.25	0.25

Table 4. Comparison with literature.

Ref	Size (mm^2)	Mutual Coupling (S_{21}) dB	Bandwidth	ECC	Efficiency	Channel Capacity Loss	Clearance area
[10]	35 × 33	−22	3.1–5	< 0.1	99	NA	35 × 16
[11]	50 × 35	> −25	3–11	< 0.004	98	NA	NA
[12]	110 × 120	−45	2.08–10	< 0.0002	NA	NA	NA
[13]	30 × 50	−20	3–10.9	< 0.06	NA	NA	NA
[14]	40 × 20	−20	2.5–11	< 0.1	NA	< 0.1	NA
[15]	24 × 32	−16	3.1–12.5	< 0.05	NA	< 0.4	NA
[16]	50 × 35	−21	1.83–13.82	< 0.059	84	< 0.35	NA
[17]	80 × 40	> −20	3.18–11.5	< 0.015	90	< 0.4	NA
[18]	39 × 17.5	−20	3.13–3.2 7.87–12.08	< 0.001	NA	NA	NA
Proposed	32 × 20	−24.42	2.6–3.5 5.66–10.8	< 0.01	94	< 0.4	32 × 20

4. CONCLUSION

A novel arbitrarily shaped antenna is designed, and it is extended to 2×2 MIMO. The proposed MIMO antenna covers two bands. Band1 covers 3–4.44 GHz, and band-2 covers from 5.32–11.1 GHz. A novel circular ring shaped NR structure is used to mitigate the effect of MC. Results from the simulation and measurements are remarkably similar. The performance of the proposed MIMO antenna is also evaluated in terms of ECC, DG, channel capacity loss, and radiation patterns. The suggested MIMO antenna is the perfect choice for UWB applications.

REFERENCES

1. Rao, P. S., K. J. Babu, and A. M. Prasad, "A multi-band multi-slot MIMO antenna with enhanced isolation," *Wireless Personal Communications*, Vol. 119, No. 3, 2239–2252, March 2021.
2. Vasu Babu, K., P. S. Rao, B. Chandrababu Naik, and B. Ravi Kumar, "Compact dual-band design and analysis of half-circular U-shape MIMO radiator for wireless applications," *Microsystem Technologies*, Vol. 29, 501–514, August 2022.
3. Tiwari, R. N., P. Singh, B. K. Kanaujia, and K. Srivastava, "Neutralization technique based two and four port high isolation MIMO antennas for UWB communication," *Int. J. Electron. Commun. (AEÜ)*, Vol. 110, October 2019.
4. Kayabasi, A., A. Toktas, E. Yigit, and K. Sabanci, "Triangular quad-port multi-polarized UWB MIMO antenna with enhanced isolation using neutralization ring," *Int. J. Electron. Commun.*, Vol. 85, 47–53, February 2017.
5. Zhang, S. and G. F. Pedersen, "Mutual coupling reduction for UWB MIMO antennas with a wide band neutralization line," *IEEE Antennas and Wireless Propagation Letters*, Vol. 15, 166–169, May 2015.
6. Najafy, V. and M. Bemani, "Mutual-coupling reduction in triple-band MIMO antennas for WLAN using CSRRs," *International Journal of Microwave and Wireless Technologies*, Vol. 12, No. 8, 762–768, March 2020.
7. Shin, H. and H. Kim, "MIMO antenna for IOT devices with reconfigurable radiation pattern," *IET Electronics Letters*, Vol. 58, No. 7, March 2022.
8. Bartoli, G., et al., "Spatial multiplexing in near field MIMO channels with reconfigurable intelligent surfaces," *IET Signal Processing*, February 2023.
9. Kaushal, V., A. Birwal, and K. Patel, "Diversity characteristics of four element ring slot-based MIMO antenna for sub-6-GHz applications," *ETRI Journal*, 1–13, 2023.
10. Khan, M. I. and M. I. Khattak, "Designing and analyzing a modern MIMO-UWB antenna with a novel stub for stop band characteristics and reduced mutual coupling," *Microwave and Optical Technology Letters*, Vol. 62, No. 10, 3209–3214, May 2020.
11. Patra, P. K. and M. K. Das, "Modified ground with $50\,\Omega$ step fed WLAN notch 2×2 MIMO UWB antenna," *Int. J. RF Microw. Comput. Aided Eng.*, Vol. 30, No. 3, March 2020.
12. Wang, L., Z. Du, H. Yang, R. Ma, Y. Zhao, X. Cui, and X. Xi, "Compact UWB MIMO antenna with high isolation using Fence-type decoupling structure," *IEEE Antennas and Wireless Propagation Letters*, Vol. 18, No. 8, 1641–1645, August 2019.
13. Zhao, X., S. Riaz, and S. Geng, "A reconfigurable MIMO/UWB MIMO antenna for cognitive radio applications," *IEEE Access*, Vol. 7, 46739–46747, April 2019.
14. Singh, H. V. and S. Tripathi, "Compact UWB MIMO antenna with cross-shaped unconnected ground stub using characteristic mode analysis," *Microwave and Optical Technology Letters*, Vol. 61, No. 7, 1874–1881, July 2019.
15. Li, W., Y. Hei, P. M. Grubb, X. Shi, and R. T. Chen, "Compact inkjet-printed flexible MIMO antenna for UWB applications," *IEEE Access*, Vol. 6, 50290–50298, September 2018.
16. Iqbal, A., O. A. Saraereh, A. W. Ahmad, and S. Bashir, "Mutual coupling reduction using F-shaped stubs in UWB-MIMO antenna," *IEEE Access*, Vol. 6, 2755–2759, December 2017.

17. Hakimi, S., S. K. Abdul Rahim, M. I. Sabran, A. N. Obadiah, and H. Mohamed, "Compact MIMO antenna for indoor UWB applications," *Microwave and Optical Technology Letters*, Vol. 58, No. 10, 2387–2393, October 2016.
18. Lin, G.-S., C.-H. Sung, J.-L. Chen, L.-S. Chen, and M.-P. Houng, "Isolation improvement in UWB MIMO antenna system using carbon black film," *IEEE Antennas and Wireless Propagation Letters*, Vol. 16, 222–225, May 2016.